Article

Fabrication of Superconducting Nb–AlN–NbN Tunnel Junctions Using Electron-Beam Lithography

Mikhail Yu. Fominsky *, Lyudmila V. Filippenko, Artem M. Chekushkin, Pavel N. Dmitriev and Valery P. Koshelets

Kotelnikov Institute of Radio Engineering and Electronics of RAS, Mokhovaya 11-7, 125009 Moscow, Russia; lyudmila@hitech.cplire.ru (L.V.F.); chekushkin@hitech.cplire.ru (A.M.C.); pavel@hitech.cplire.ru (P.N.D.); valery@hitech.cplire.ru (V.P.K.)
* Correspondence: demiurge@hitech.cplire.ru; Tel.: +7-495-6293418

Abstract: Mixers based on superconductor–insulator–superconductor (SIS) tunnel junctions are the best input devices at frequencies from 0.1 to 1.2 THz. This is explained by both the extremely high nonlinearity of such elements and their extremely low intrinsic noise. Submicron tunnel junctions are necessary to realize the ultimate parameters of SIS receivers, which are used as standard devices on both ground and space radio telescopes around the world. The technology for manufacturing submicron Nb–AlN–NbN tunnel junctions using electron-beam lithography was developed and optimized. This article presents the results on the selection of the exposure dose, development time, and plasma chemical etching parameters to obtain high-quality junctions (the ratio of the resistances below and above the gap R_j/R_n). The use of a negative-resist ma-N 2400 with lower sensitivity and better contrast in comparison with a negative-resist UVN 2300-0.5 improved the reproducibility of the structure fabrication process. Submicron (area from 2.0 to 0.2 μm^2) Nb–AlN–NbN tunnel junctions with high current densities and quality parameters $R_j/R_n > 15$ were fabricated. The spread of parameters of submicron tunnel structures across the substrate and the reproducibility of the cycle-to-cycle process of tunnel structure fabrication were measured.

Keywords: electron-beam lithography; negative electronic resists; plasma chemical etching; magnetron sputter deposition; superconducting tunnel structures; niobium-based high-quality tunnel junctions

Citation: Fominsky, M.Y.; Filippenko, L.V.; Chekushkin, A.M.; Dmitriev, P.N.; Koshelets, V.P. Fabrication of Superconducting Nb–AlN–NbN Tunnel Junctions Using Electron-Beam Lithography. *Electronics* **2021**, *10*, 2944. https://doi.org/10.3390/electronics10232944

Academic Editor: Elias Stathatos

Received: 31 October 2021
Accepted: 22 November 2021
Published: 26 November 2021

Publisher's Note: MDPI stays neutral with regard to jurisdictional claims in published maps and institutional affiliations.

Copyright: © 2021 by the authors. Licensee MDPI, Basel, Switzerland. This article is an open access article distributed under the terms and conditions of the Creative Commons Attribution (CC BY) license (https://creativecommons.org/licenses/by/4.0/).

1. Introduction

One of the most successful areas of superconducting electronics is the development of low-noise terahertz receivers [1,2]. The development of terahertz technologies and the creation of SIS receivers with quantum sensitivity and THz radiation sources for use in space- and ground-based radio telescopes are important tasks. Mixers based on SIS tunnel junctions are the best input devices at frequencies f from 0.1 to 1.2 THz; their noise temperatures are limited only by the quantum value hf/k_B, where h and k_B are the Plank and Boltzmann constants, respectively [1–3]. Currently, heterodyne SIS receivers are used as standard devices on most ground-based and space radio telescopes around the world [4,5]. To implement the ultimate parameters of SIS mixers, it is necessary to create and optimize a reproducible and reliable technology for the fabrication of nanostructures with a tunnel barrier thickness on the order of 1 nm with an extremely high current density and low leakage currents [6–8]. For operation at frequencies below 1 THz, tunnel junctions with very high tunnel barrier transparencies are required. For the AlO_x barrier, there is a transparency limit corresponding to a current density of about 10–15 kA/cm^2; at a higher current density, the quality of the tunnel junction degrades significantly. The problem was overcome by developing Nb–AlN–Nb tunnel junctions with rather good $R_j/R_n > 15$ at very high current densities up to 100 kA/cm^2 [9,10]. Replacing an Nb counter electrode with an

NbN provides a significant improvement in the performance of the Nb–AlN–NbN SIS THz mixer due to the much higher gap voltages [7,8]. To match the waveguide elements of the high-current-density mixer with the receiving antenna, the area of the SIS junctions must be substantially less than a square micrometer. Electron-beam lithography is one of the most promising methods for the fabrication of nanostructures for research purposes since it allows, within a short time, changing the design of both single selected elements and the entire microcircuit and achieving high reproducibility in the submicron region of tunnel junctions [11,12].

This article describes the technology of SIS tunnel structure fabrication of submicron sizes using direct electron-beam lithography (EBL) and subsequent plasma chemical etching for the manufacture of high-quality tunnel structures with good reproducibility and minimal deviation of parameters along the substrate. The SIS junction on silicon or quartz substrate was formed by etching a three-layer Nb–AlN–NbN structure through a resist mask formed using EBL. After fabrication of the tunnel junction using plasma chemical etching, anodizing was carried out, and then an insulation layer of SiO_2 was applied [13]. In the final stages, the counter NbN electrode and Au contact pads were formed. Each step in the manufacturing of tunnel junctions was inspected using electron microscopy. Several series of Nb–AlN–NbN tunnel junctions of submicron sizes with a current density of 20 to 50 kA/cm^2 were fabricated. The reproducibility of the parameters of tunnel junctions of submicron sizes over the substrate and the reproducibility of the process of fabricating structures from cycle to cycle are demonstrated. The measurements were carried out using an automated system for measuring the current–voltage characteristics and electrophysical parameters of the SIS tunnel junctions IRTECON [14].

2. Materials and Methods

2.1. Sputtering Equipment and Technology Processes

The three-layer Nb–AlN–NbN structure was deposited using two high-vacuum sputtering plants: Kurt Lesker and Leybold L560UV (Leybold, Köln, Germany). The Leybold L560UV is equipped with a water-cooled substrate holder, as well as two direct-current (DC) and high-frequency (RF) magnetron sputtering systems. Kurt Lesker is a two-chamber cluster system with a chamber equipped with four DC and two RF magnetron sputtering systems, as well as an oxidation/nitridization chamber with an electron ion gun. The base niobium electrode and a thin layer of aluminum were deposited by DC magnetron sputtering in an argon atmosphere. After the deposition of the barrier aluminum, the substrate was placed over an RF magnetron, on which a target with aluminum was attached, and a plasma discharge was initiated in a nitrogen atmosphere [15]. The choice of the AlNx barrier is due to the fact that the AlOx barrier degrades at RnS values of about 20 $\Omega\cdot\mu m^2$ or less, which leads to a deterioration in the current–voltage characteristics [16]. Another important advantage of the AlNx barrier is the possibility of using NbN as the counter electrode of the tunneling structure, which makes it possible to increase the gap voltage of the junction to 3.7 mV, thereby significantly increasing the upper frequency limit of the operation of microwave devices [17]. At the end of the nitridization process, the counter NbN electrode was deposited on the tunnel barrier, which was formed by DC magnetron sputtering in argon and nitrogen. The workflow for the formation of the three-layer structure is shown in Table 1.

Table 1. Formation of the three-layer structure in a single vacuum cycle (Leybold L560UV).

Material	Description	Thickness, nm	Deposition Parameters
Nb	Base electrode	200	DC, 600 W, Ar, 4 mTorr, 1.8 nm/s
Al	Tunnel barrier	6	DC, 100 W, Ar, 3 mTorr, 0.13 nm/s
AlN	Tunnel barrier	1.0–1.2	RF, 70 W, N2, 0.03 mTorr
NbN	Counter electrode	80	DC, 600 W, Ar + N2, 4 mTorr, 1.4 nm/s

The fabrication procedure given in the Table 1 was the same as for Nb/AlN/Nb junctions except for the NbN counter electrode [8]. The NbN film was deposited by DC reactive magnetron sputtering using an Ar + 9% N_2 gas mixture.

2.2. Electron-Beam Lithography

To study the manufacturing process of submicron junctions, test samples were prepared. The array of circular structures was formed in various modes of electron-beam exposure, development, and plasma chemical etching, as shown in Figure 1, separated by a distance exceeding the proximity effect [12]. To avoid possible problems with the resist heating effect, a minimum aperture and a defocused beam were used for exposure [18,19].

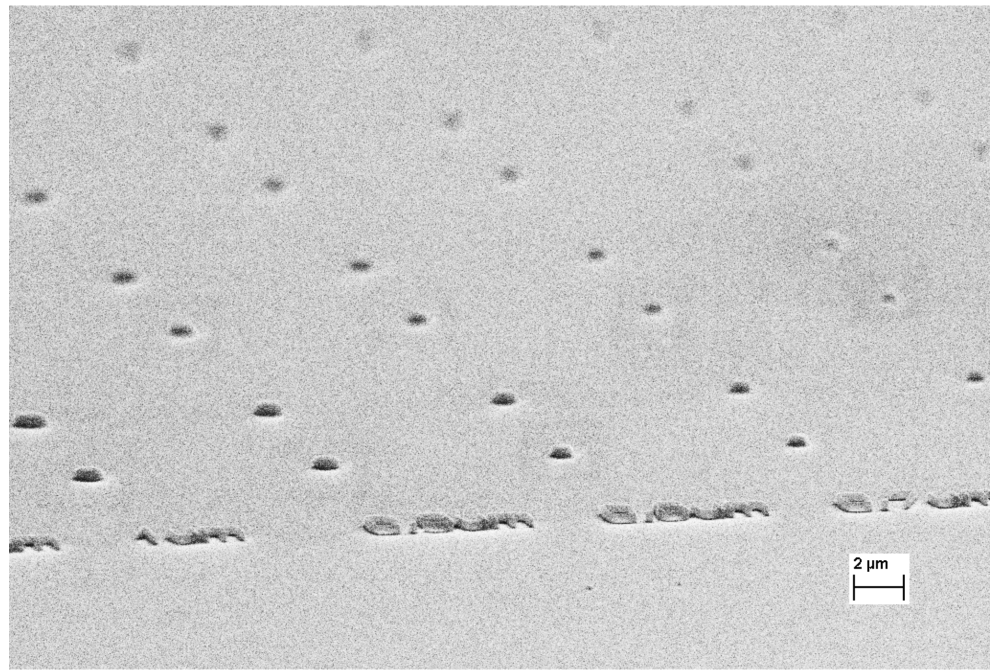

Figure 1. Array of structures for testing the process of fabrication submicron-sized tunnel junctions. The sample was located at an angle to the axis of the electron microscope probe.

Various types of negative resist were used to shape the geometry of the tunnel junctions. The negative resist UVN 2300-0.5 is characterized by high sensitivity and is used for both photolithography (DUV, 248 nm) and electron-beam lithography [20,21]. The negative electronic resist UVN 2300-0.5 was deposited on the already formed three-layer Nb–AlN–NbN structure. The resist was then baked at 90 °C for 10 min. The thickness of the resistive film was 0.38 µm. Electron-beam exposure was carried out on a Raith e_Line electron lithography system with an accelerating voltage of 30 keV; the resist dose was varied depending on the junction size, ranging from 8 to 20 $\mu C/cm^2$ [22,23]. After exposure, the samples were baked at 110 °C for 10 min. Unexposed resist areas were then removed in a 2.4% solution of tetramethylammonium hydroxide pentahydrate (TMAH). The negative resist UVN 2300-0.5 has a low contrast; thus, the technological process is quite sensitive to deviations, which affects the reproducibility of the results. When using the UVN 2300-0.5 resist, the doses for tunnel junctions were selected depending on the size of the tunnel junction: a dose of 10 $\mu C/cm^2$ is optimal for structures with dimensions of 2.0 and 1.5 µm; a dose of 15 $\mu C/cm^2$ is optimal for structures 0.7–1.0 µm; a dose of 20 $\mu C/cm^2$ is optimal for structures 0.4–0.6 µm. Thus, tunnel junctions with an area of up to 0.15 μm^2 were fabricated and measured.

To increase the reproducibility of the technology for manufacturing tunnel junctions, the electronic resist ma-N 2400 was tested [24]. The negative resist ma-N 2400 is used for both photolithography (DUV, 248 nm) and electron-beam lithography, but the sensitivity

of this resist is an order of magnitude lower than that of UVN 2300-0.5; therefore, for structures with submicron sizes, the resolution of ma-N 2400 will be higher. A negative e-beam resist ma-N 2400 was deposited on an already formed three-layer Nb–AlN–NbN structure. After application, the resist was baked at 90 °C for 3 min. The dose for EBL was varied, ranging from 110 to 275 μC/cm^2. The unexposed areas of the resist were removed in 2.4% TMAH solution.

To increase the resistance of the resistive mask to etching, the samples were heated to 100 °C for 10 min after development [25].

2.3. Plasma Chemical Etching

Tunnel junctions were formed by plasma chemical etching of NbN over a resist mask using two different plasma chemical etching plants: in the vacuum chamber of a Secon XPE II plasma chemical etching unit in an SF_6 atmosphere (Figure 2) and in a mixture of O_2 and CF_4 gases using a March Jupiter II plasma chemical etching unit (Figure 3). An additional NbN sample, identical in thickness and geometry to the main Nb–AlN–NbN sample, was placed in the plasma chemical etching unit to control the etching process [26]. The etching time of the NbN layer was determined from the etching process of this NbN test sample and ranged from 100 to 120 s. After the NbN layer visually disappeared on this NbN test sample, the Nb–AlN–NbN sample was etched for an additional 15% of the etching time, since the thin NbN layer was visually transparent. For the Nb–AlN–NbN sample, the etching process stopped at the AlN layer, which is the stop layer for the etching process. To achieve high reproducibility and small deviations of parameters, the etching process was studied, and the optimal conditions for anisotropic chemical etching of the NbN film with a minimum reproducible undercut were found. For plasma chemical etching on a Secon XPE II unit in an SF_6 atmosphere, the following parameters were used: isotropic plasma chemical etching (PE); power, 200 W; flow SF_6, 10 sccm; pressure, 2.0×10^{-1} mbar.

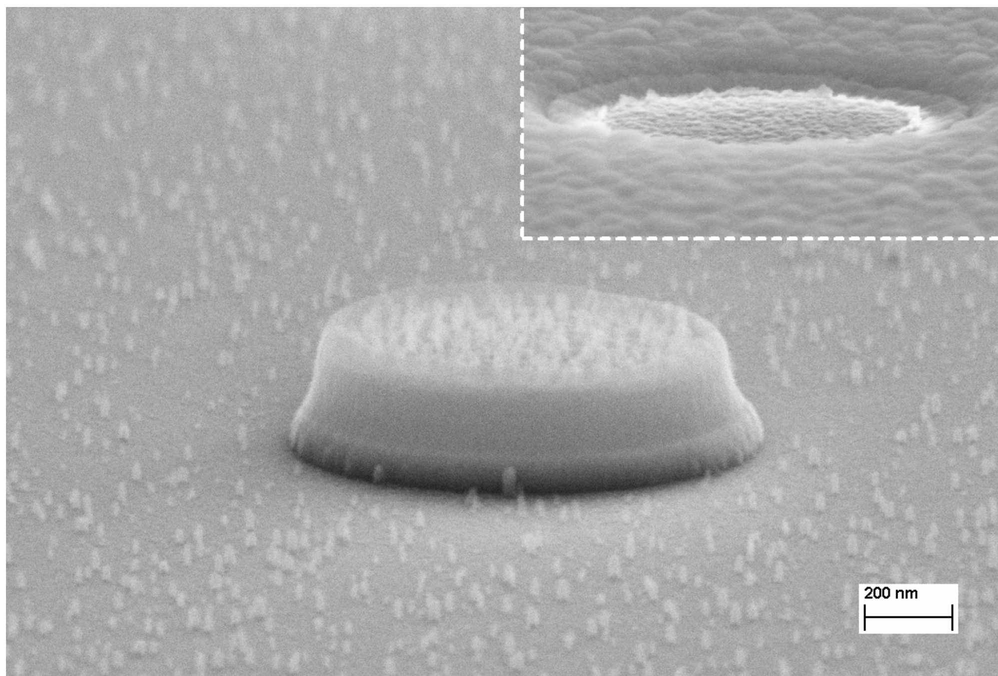

Figure 2. The ma-N 2400 resist film with a diameter of 1 μm, exposed at a dose of 275 μC/cm^2 after plasma chemical etching in an SF_6 atmosphere. The diameter of the NbN layer of the three-layer structure is 1.02 μm corresponding to the planned size. Inset in the upper-right corner: tunnel junction after applying SiO_2 insulation and liftoff.

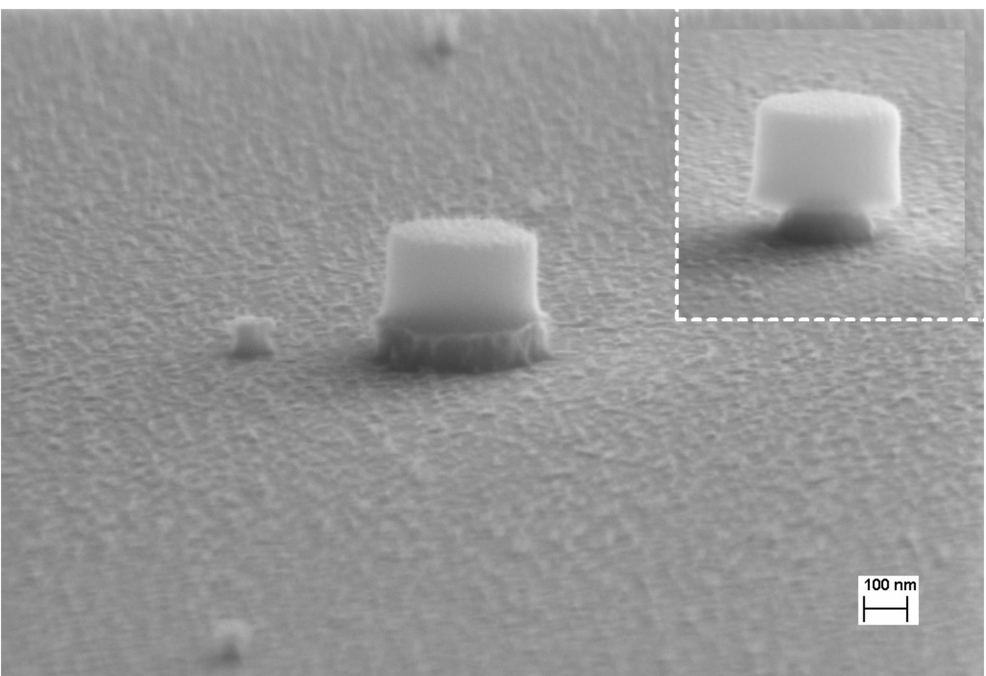

Figure 3. The ma-N 2400 resist film with a diameter of 0.4 μm, exposed at a dose of 275 μC/cm^2 after plasma chemical etching in a CF_4 atmosphere. Inset in the upper-right corner: the sample after etching in the CF_4 + O_2 atmosphere with nonoptimal parameters. In both cases, the diameter of the resist after etching was 0.33 μm.

Figure 4 shows photographs taken from an electron microscope for a UVN 2300-0.5 sample with a diameter of 0.4 μm. The resist profile was significantly different from the vertical axis (insufficient contrast UVN 2300-0.5); the diameters of the resistive mask and three-layer structure differed significantly from the design size.

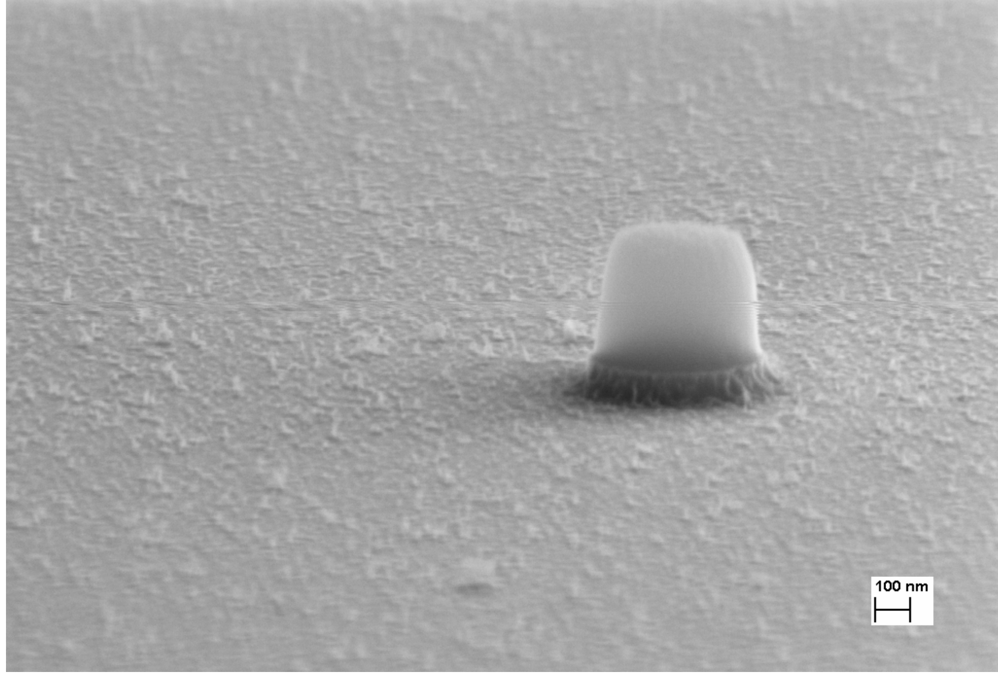

Figure 4. The UVN 2300-0.5 test sample with a diameter of 0.4 μm, exposed at a dose of 20 μC/cm^2 after plasma chemical etching with a resist mask in a CF_4 atmosphere. The diameter of the resistive mask after etching was 0.46 μm; the diameter of the three-layer structure was 0.51 μm.

2.4. Anodization

After plasma chemical etching, anodization was carried out in an electrolyte solution of ammonium tetraborate with glycol; as a result, the niobium nitride film, not covered by the resist, was transformed into anodic oxide [27]. Anodization was carried out up to a voltage of 8–10 V at currents of 100–200 μA. Next, a layer of SiO_2 insulator was applied (Figure 2).

The final technological stages were the formation of the counter NbN electrode and Au contact pads using photolithography with a AZ 5214 photoresist (Figure 5).

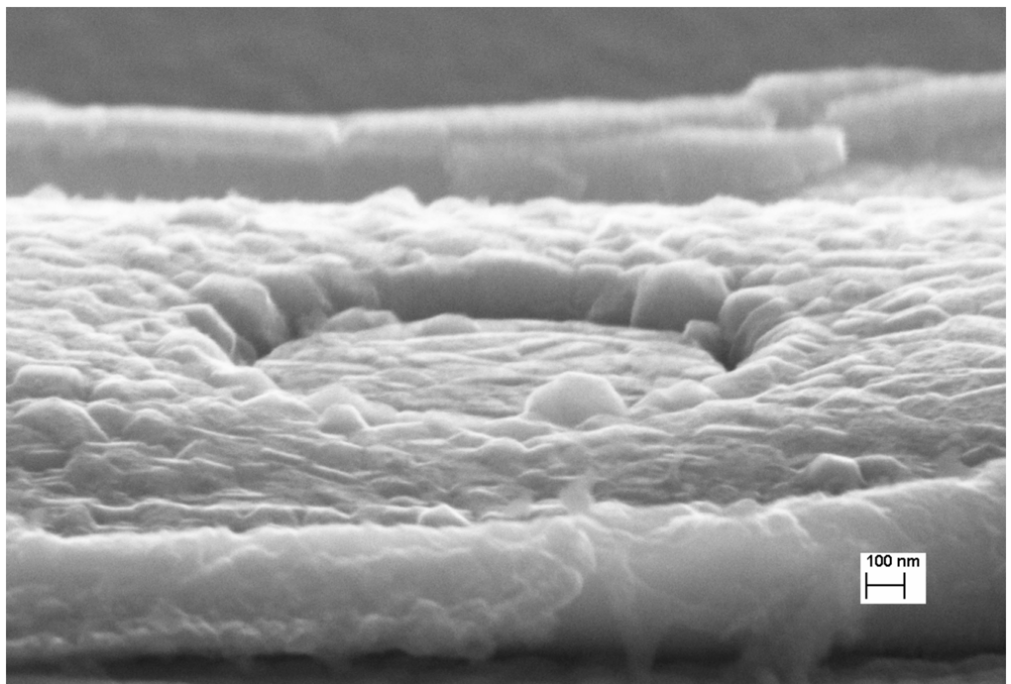

Figure 5. SEM photo of the SIS junction after deposition of the counter NbN electrode.

3. Experimental Results

Several series of Nb–AlN–NbN tunnel junctions of submicron sizes with a current density of 20 to 50 kA/cm^2 were fabricated.

The use of the negative resist ma-N 2400 (solid line in Figure 6), with lower sensitivity and better contrast in comparison with UVN 2300-0.5, increased the reproducibility of the tunnel junction fabrication process.

The negative-resist ma-N 2400 had a sensitivity that was one order of magnitude lower than that of UVN 2300-0.5 and had a better contrast. As can be seen from the measurement data (solid curves in Figure 6), for exposure doses of 220 and 275 $\mu C/cm^2$, the size drifts were constant (in contrast to the UVN 2300-0.5 resist) and were practically absent in the entire measurement range from 1.0 to 0.1 μm.

To achieve high reproducibility and small deviations of parameters, the plasma chemical etching process was studied using electron microscopy, and the optimal conditions for anisotropic chemical etching of the NbN film with a minimum reproducible undercut were found (Figure 7). Etching in an SF_6 atmosphere showed better reproducibility of structures from cycle to cycle with higher-quality tunnel junctions.

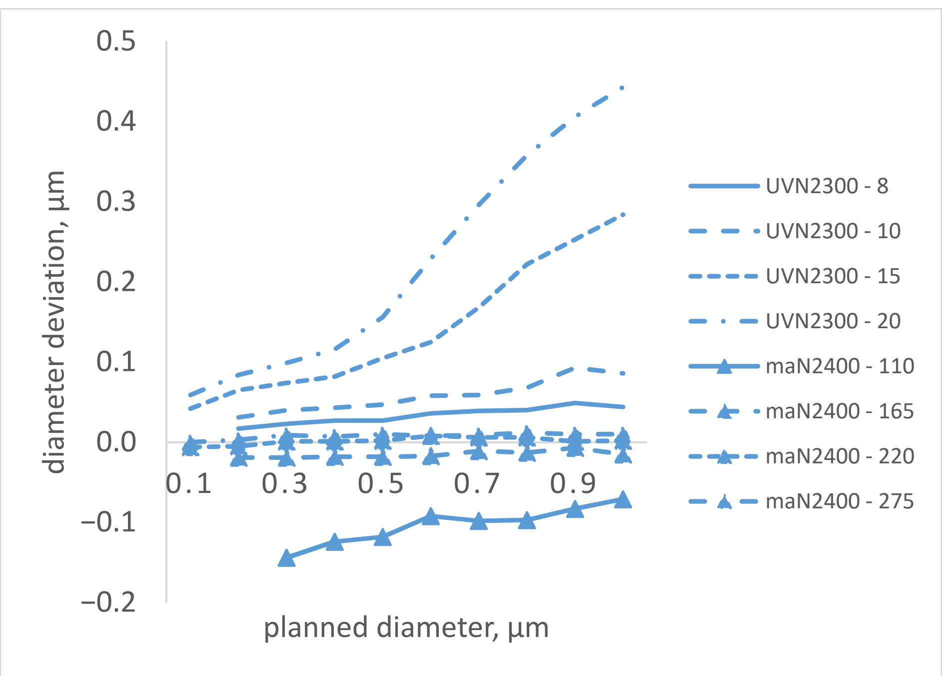

Figure 6. Deviation of the size of tunnel junctions during exposure and development (TMAH 2.4%, time 60 s) for ma-N 2400 and UVN 2300-0.5 resists. The horizontal axis is the planned diameter. The vertical axis is the difference in the diameter of the structures measured with an electron microscope minus the design value. Positive values correspond to a larger diameter than planned.

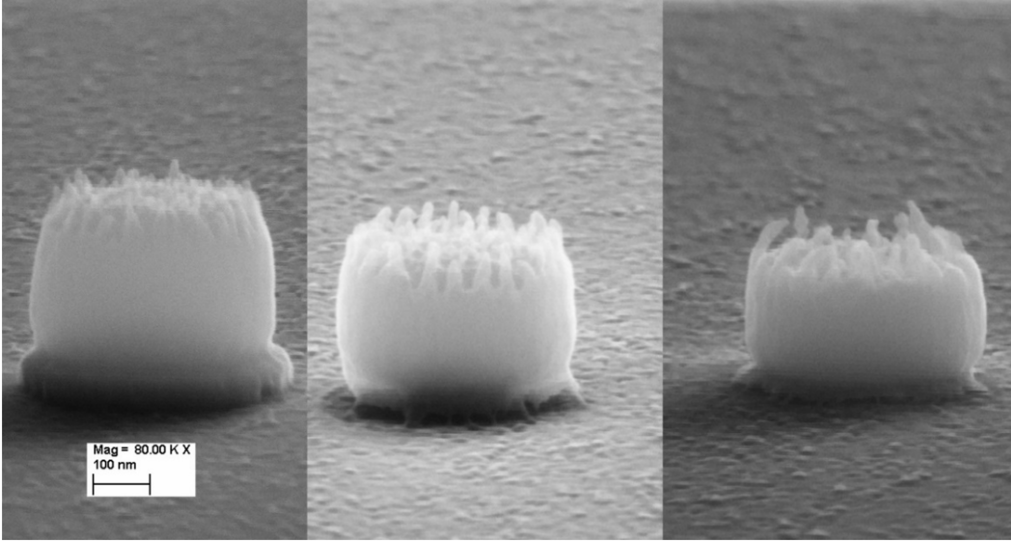

Figure 7. Plasma chemical etching of samples in an SF_6 atmosphere. For the left sample, the etching time was 30 s; for the sample in the center, it was 45 s; for the right sample, it was 60 s.

The measurements were carried out using an automated system for measuring the current–voltage characteristics and electrophysical parameters of the SIS tunnel junctions IRTECON [14]. A data acquisition system for the Integrated Receiver Test and Control (IRTECON) was developed for automated measurements and control of a single-chip superconducting integrated receiver for the Terahertz Limb Sounder (TELIS) balloon project intended to measure a variety of stratosphere trace gases [28]. The IRTECON system was used in many laboratories over the world to study and control the SIS receivers, particularly for advanced tuning and diagnostic of the ALMA Band 5 receiver channel [29].

For the current–voltage characteristics of Nb–AlN–NbN tunnel junctions of the same size, located both on different substrates and on different parts of the same substrate, similar parameters were demonstrated. Figure 8 shows the I–V characteristics of Nb–AlN–NbN tunnel junctions of the same size, located on different parts of the same substrate.

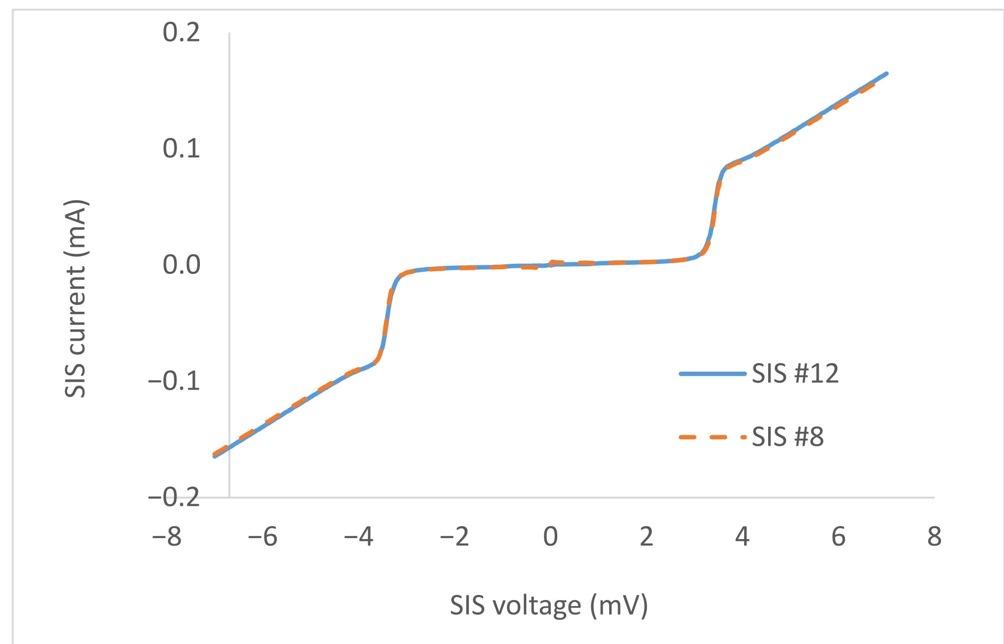

Figure 8. I–V characteristics of Nb–AlN–NbN junctions of the same size, fabricated using EBL and plasma chemical etching in a CF_4 atmosphere, located on different parts of the same substrate: SIS #8 with an area of 0.480 μm^2 with a current density of 15 kA/cm^2, R_n = 40.98 Ω, R_j/R_n = 18.4, V_g = 3.39 mV; SIS #12 with an area of 0.488 μm^2 with a current density of 15 kA/cm^2, R_n = 40.34 Ω, R_j/R_n = 20.7, V_g = 3.38 mV.

The measurements were carried out on tunnel junctions with an area of up to 0.15 μm^2; the quality of the junctions did not degrade with decreasing sizes (Figure 9). Figure 10 shows the I–V characteristics of Nb–AlN–NbN tunnel junctions of the same size located on different substrates.

To realize a quantum-limited performance of the SIS mixers at sub-THz frequencies, tunnel junctions with very high tunnel current density are required. To achieve proper matching between such junctions and the receiving antenna, submicron SIS junctions were implemented [28,30–33]. SIS mixers have already been successfully used for both space missions and ground-based telescopes (TELIS, CHAMP) [7,30–32]. Up to now, SIS junctions with an area down to 0.5 μm^2 have been fabricated by conventional photolithography processes. To improve the performance and the yield of SIS mixers and to ensure equality of the SIS junctions in the twin mixer circuits [32,33], implementation of electron-beam lithography is highly desirable. This is especially important for the development of SIS array receivers and the further increase in the SIS operating frequency above 1 THz.

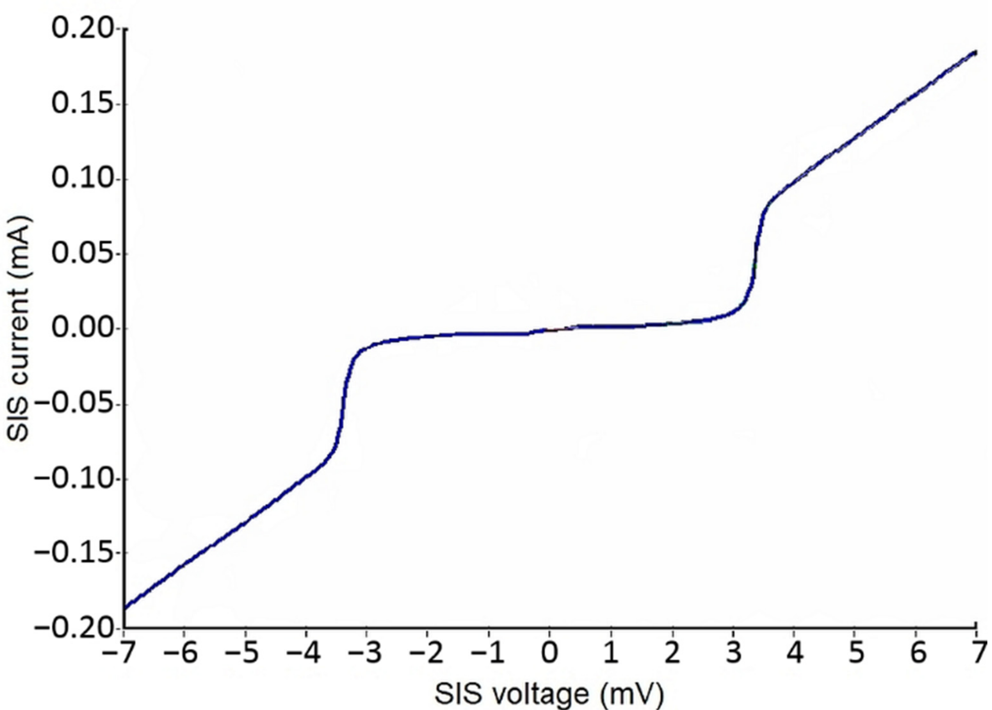

Figure 9. I–V characteristics of the Nb–AlN–NbN junction with an area of 0.15 μm^2 with a current density of 47 kA/cm^2, R_n = 34.53 Ω, R_j/R_n = 21.1, V_g = 3.36 mV fabricated using EBL and plasma chemical etching in a CF_4 atmosphere.

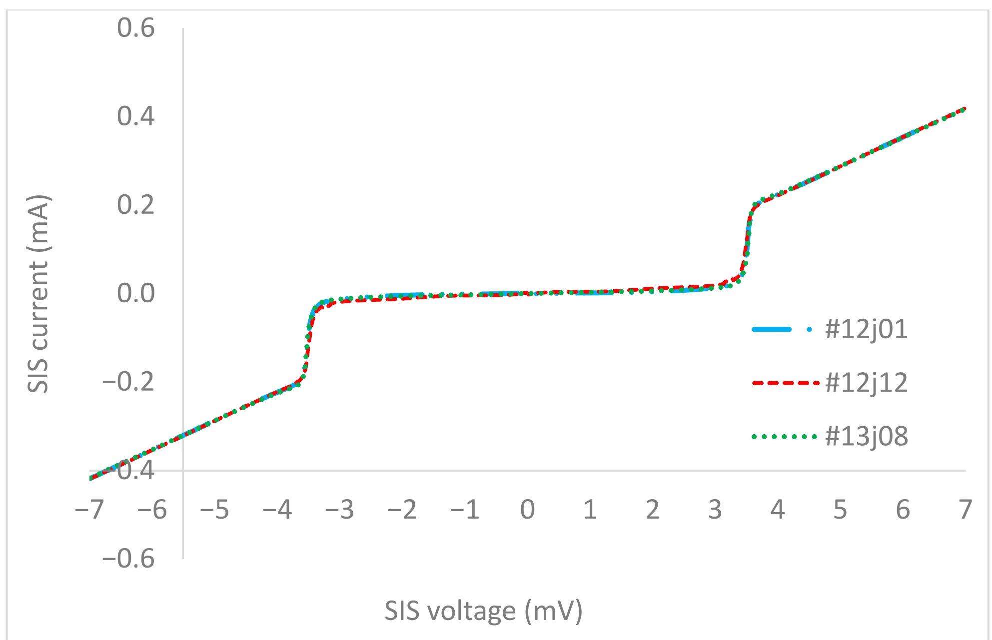

Figure 10. I–V characteristics of Nb–AlN–NbN junctions of the same size, fabricated using EBL and plasma chemical etching in an SF_6 atmosphere, located both on different substrates and on different parts of the same substrate: SIS #12j01 (area 0.732 μm^2 with a current density of 25 kA/cm^2, R_n = 15.22 Ω, R_j/R_n = 38.1, V_g = 3.51 mV); SIS #12j12 (area 0.735 μm^2 with a current density of 23.2 kA/cm^2, R_n = 15.16 Ω, R_j/R_n = 13.2, V_g = 3.49 mV); SIS #13j08 (area 0.743 μm^2 with a current density of 24.5 kA/cm^2, R_n = 15.44 Ω, R_j/R_n = 23.4, V_g = 3.52 mV).

4. Conclusions

The technology for the fabrication of submicron Nb–AlN–NbN tunnel junctions using EBL lithography was developed and optimized. The use of a negative-resist ma-N 2400 with lower sensitivity and better contrast in comparison with a negative resist UVN 2300-0.5 improved the reproducibility of the tunnel junction fabrication process from cycle to cycle. A high-quality ultrathin AlN barrier was formed during the nitridization of the Al surface in RF plasma discharge in a pure N_2 atmosphere. Etching in an SF_6 atmosphere showed better reproducibility of structures from cycle to cycle with higher-quality tunnel junctions. As a result, Nb–AlN–NbN tunnel junctions of submicron sizes were fabricated with a high current density and a quality parameter $R_j/R_n > 15$ (area from 2.0 to 0.2 μm^2). To implement the ultimate parameters of SIS mixers and to ensure equality of the SIS junctions in the twin mixer circuits, further implementation of electron-beam lithography is highly desirable. This is especially important for the development of SIS array receivers and the further increase in the SIS operating frequency above 1 THz.

Author Contributions: Conceptualization, V.P.K.; methodology, M.Y.F., L.V.F., A.M.C. and P.N.D.; electron-beam lithography, M.Y.F.; sputtering, L.V.F., A.M.C. and P.N.D.; plasma chemical etching, M.Y.F., L.V.F., A.M.C. and P.N.D.; tunnel barrier measurements, M.Y.F. and V.P.K.; data analysis, M.Y.F. and V.P.K.; writing and editing, M.Y.F., A.M.C. and V.P.K.; funding acquisition, V.P.K. All authors have read and agreed to the published version of the manuscript.

Funding: The developments of the Nb–AlN–NbN technology and EBL process were supported by the Russian Science Foundation (project No. 19–19–00618). This work was supported by the State Assignment of the Kotelnikov IRE RAS (project No. 0030–2019–0003). The equipment of USU "Cryointegral" was used to carry out the research; USU is supported by a grant from the Ministry of Science and Higher Education of the Russian Federation, agreement No. 075-15-2021-667.

Institutional Review Board Statement: Not applicable.

Informed Consent Statement: Not applicable.

Data Availability Statement: Not applicable.

Conflicts of Interest: The authors declare no conflict of interest.

References

1. Zmuidzinas, J.; Richards, P.L. Superconducting detectors and mixers for millimeter and submillimeter astrophysics. *Proc. IEEE* **2004**, *92*, 1597–1616. [CrossRef]
2. Sizov, F.; Rogalski, A. THz detectors. *Prog. Quantum Electron.* **2010**, *34*, 278–347. [CrossRef]
3. Richards, P.L.; Shen, T.M.; Harris, R.E.; Lloyd, F.L. Quasiparticle heterodyne mixing in SIS tunnel junctions. *Appl. Phys. Lett.* **1979**, *34*, 345–347. [CrossRef]
4. Jackson, B.D.; De Lange, G.; Zijlstra, T.; Kroug, M.; Kooi, J.W.; Stern, J.A.; Klapwijk, T. Low-noise 0.8–0.96- and 0.96–1.12-THz superconductor-insulator-superconductor mixers for the herschel space observatory. *IEEE Trans. Microw. Theory Tech.* **2006**, *54*, 547–558. [CrossRef]
5. Karpov, A.; Miller, D.; Rice, F.; Stern, J.A.; Bumble, B.; LeDuc, H.G.; Zmuidzinas, J. Low Noise 1 THz–1.4 THz Mixers Using Nb/Al-AlN/NbTiN SIS Junctions. *IEEE Trans. Appl. Supercond.* **2007**, *17*, 343–346. [CrossRef]
6. Rudakov, K.I.; Koshelets, V.P.; Baryshev, A.M.; Dmitriev, P.N.; Khudchenko, A.V. The 700–950 GHz Superconducting Receiving Structures for Radio Astronomy. *Radiophys. Quantum Electron.* **2017**, *59*, 711–714. [CrossRef]
7. Torgashin, M.Y.; Koshelets, V.P.; Dmitriev, P.N.; Ermakov, A.B.; Filippenko, L.V.; Yagoubov, P.A. Superconducting Integrated Receiver Based on Nb-AlN-NbN-Nb Circuits. *IEEE Trans. Appl. Supercond.* **2007**, *17*, 379–382. [CrossRef]
8. Dmitriev, P.N.; Lapitskaya, I.L.; Filippenko, L.V.; Ermakov, A.B.; Shitov, S.; Prokopenko, G.V.; Kovtonyuk, S.A.; Koshelets, V. High quality Nb-based tunnel junctions for high frequency and digital applications. *IEEE Trans. Appl. Supercond.* **2003**, *13*, 107–110. [CrossRef]
9. Shiota, T.; Imamura, T.; Hasuo, S. Nb Josephson junction with an AlNx barrier made by plasma nitridation. *Appl. Phys. Lett.* **1992**, *61*, 1228–1230. [CrossRef]
10. Kawamura, J.; Miller, D.; Chen, J.; Zmuidzinas, J.; Bumble, B.; LeDuc, H.G.; Stern, J.A. Very high-current-density Nb/AlN/Nb tunnel junctions for low-noise submillimeter mixers. *Appl. Phys. Lett.* **2000**, *76*, 2119–2121. [CrossRef]
11. Chen, Y. Nanofabrication by electron beam lithography and its applications: A review. *Microelectron. Eng.* **2015**, *135*, 57–72. [CrossRef]
12. Chang, T.H.P. Proximity effect in electron-beam lithography. *J. Vac. Sci. Technol.* **1975**, *12*, 1271–1275. [CrossRef]

13. Rudakov, K.I.; Dmitriev, P.N.; Baryshev, A.M.; Khudchenko, A.V.; Hesper, R.; Koshelets, V.P. Low-Noise Sis Receivers for New Radio-Astronomy Projects. *Radiophys. Quantum Electron.* **2019**, *62*, 547–555. [CrossRef]
14. Ermakov, A.B.; Shitov, S.V.; Baryshev, A.M.; Koshelets, V.P.; Luinge, W. A data acquisition system for test and control of superconducting integrated receivers. *IEEE Trans. Appl. Supercond.* **2001**, *11*, 840–843. [CrossRef]
15. Bumble, B.; LeDuc, H.G.; Stern, J.A.; Megerian, K.G. Fabrication of Nb/Al-N/sub x//NbTiN junctions for SIS mixer applications. *IEEE Trans. Appl. Supercond.* **2001**, *11*, 76–79. [CrossRef]
16. Kleinsasser, A.W.; Miller, R.E.; Mallison, W.H.; Arnold, G.B. Observation of multiple Andreev reflections in superconducting tunnel junctions. *Phys. Rev. Lett.* **1994**, *72*, 1738–1741. [CrossRef]
17. Iosad, N.N.; Balashov, D.V.; Kupriyanov, M.Y.; Polyakov, S.N.; Roddatis, V.V. Characterization of NbN/AlN/NbN tunnel junctions fabricated without intentional heating. *IEEE Trans. Appl. Supercond.* **1997**, *7*, 2805–2808. [CrossRef]
18. Abe, T.; Ohta, K.; Wada, H.; Takigawa, T. Resist heating effect in direct electron beam writing. *J. Vac. Sci. Technol. B Microelectron. Nanometer Struct.* **1988**, *6*, 853. [CrossRef]
19. Saito, K.; Sakai, T. Criterion to judge whether the resist heating effect will occur. *J. Vac. Sci. Technol. B Microelectron. Nanometer Struct.* **1991**, *9*, 3464. [CrossRef]
20. Distribution DOW Products. Available online: https://www.microresist.de/en/?jet_download=6982 (accessed on 31 October 2021).
21. Niepce, D. Fabrication and Characterisation of Thin-Film Superconducting Nanowire Superinductors for Novel Quantum Devices. Master's Thesis, Chalmers University of Technology, Goteborg, Sweden, 2014.
22. Nanoengineering EBL Tool: eLINE Plus | Raith Group. Available online: https://www.raith.com/product/eline-plus/ (accessed on 18 November 2021).
23. Greve, M.M.; Holst, B. Optimization of an electron beam lithography instrument for fast, large area writing at 10 kV acceleration voltage. *J. Vac. Sci. Technol. B* **2013**, *31*, 043202. [CrossRef]
24. Elsner, H.; Meyer, H.-G.; Voigt, A.; Grützner, G. Evaluation of ma-N 2400 series DUV photoresist for electron beam exposure. *Microelectron. Eng.* **1999**, *46*, 389–392. [CrossRef]
25. Negative Tone Photoresist Series ma-N 2400. Available online: https://www.nanophys.kth.se/nanolab/resists/ma-N240X-pdfs/vh_man_2400_en_07030504_ls.pdf (accessed on 31 October 2021).
26. Filippenko, L.V.; Shitov, S.; Dmitriev, P.N.; Ermakov, A.B.; Koshelets, V.; Gao, J.-R. Submillimeter superconducting integrated receivers: Fabrication and yield. *IEEE Trans. Appl. Supercond.* **2001**, *11*, 816–819. [CrossRef]
27. Meng, X.; Van Duzer, T. Light-anodization process for high-J/sub c/micron and submicron superconducting junction and integrated circuit fabrication. *IEEE Trans. Appl. Supercond.* **2003**, *13*, 91–94. [CrossRef]
28. Koshelets, V.P.; Ermakov, A.B.; Filippenko, L.V.; Khudchenko, A.V.; Kiselev, O.S.; Sobolev, A.S.; Torgashin, M.Y.; Yagoubov, P.A.; Hoogeveen, R.W.M.; Wild, W. Superconducting Integrated Submillimeter Receiver for TELIS. *IEEE Trans. Appl. Supercond.* **2007**, *17*, 336–342. [CrossRef]
29. Belitsky, V.; Lapkin, I.; Fredrixon, M.; Meledin, D.; Sundin, E.; Billade, B.; Ferm, S.-E.; Pavolotsky, A.; Rashid, H.; Strandberg, M.; et al. SEPIA—A new single pixel receiver at the APEX telescope (Corrigendum). *Astron. Astrophys.* **2018**, *620*, C2. [CrossRef]
30. De Lange, G.; Birk, M.; Boersma, D.; Dercksen, J.; Dmitriev, P.; Ermakov, A.B.; Filippenko, L.V.; Golstein, H.; Hoogeveen, R.W.M.; De Jong, L.; et al. Development and characterization of the superconducting integrated receiver channel of the TELIS atmospheric sounder. *Supercond. Sci. Technol.* **2010**, *23*. [CrossRef]
31. Koshelets, V.P.; Tarasov, M.A. Superconducting terahertz receivers for space-borne and balloon-borne radio telescopes. *Bull. Russ. Acad. Sci. Phys.* **2016**, *80*, 471–475. [CrossRef]
32. Khudchenko, A.; Baryshev, A.M.; Rudakov, K.I.; Dmitriev, P.M.; Hesper, R.; De Jong, L.; Koshelets, V. High-Gap Nb-AlN-NbN SIS Junctions for Frequency Band 790–950 GHz. *IEEE Trans. Terahertz Sci. Technol.* **2015**, *6*, 127–132. [CrossRef]
33. Rudakov, K.I.; Khudchenko, A.V.; Filippenko, L.V.; Paramonov, M.E.; Hesper, R.; Lima, D.A.R.d.C.; Baryshev, A.M.; Koshelets, V.P. THz Range Low-Noise SIS Receivers for Space and Ground-Based Radio Astronomy. *Appl. Sci.* **2021**, *11*, 10087. [CrossRef]